

How large can be SDW and CDW amplitudes in underdoped cuprates

M. Eremin¹, S. Varlamov^{1,2}, and I. Eremin¹

¹Kazan State University, 420008 Kazan, Russian Federation ,

²Cottbus Technical University, 03013 Cottbus, Germany

(November 19, 2013)

Self-consistent calculation of spin (charge) density wave order (SDW/CDW) parameters have been performed for bilayered cuprates on the basis of a singlet correlated band model. Evolution of the Fermi surface in the strongly underdoped regime is described by using a two-band approach. The smooth development of the pseudogap formation temperature is explained from underdoped to overdoped states and the Fourier amplitudes $\langle s_q \rangle$ (spin) and $\langle e_q \rangle$ (charge) modulations have been calculated. We have found a maximum of the incommensurability for doping $0.09 \div 0.11$ holes per copper site.

I. INTRODUCTION

Our calculations were motivated in part by NMR experiments searching the spatial inhomogeneity of charge and spin density distributions in underdoped cuprates [1]. These investigations are connected with the very important problem of high-temperature superconductivity because the nature of a pseudogap is not completely understood. Therefore we continue our previous examination of the singlet correlated band model for layered cuprates [2] with respect to its ability to describe the observed doping dependence of a pseudogap formation temperature [3,4] and Fermi surface evolution [5].

II. BASIC RELATIONS FOR ONE BAND APPROACH

We start from the Hamiltonian:

$$H = \sum t_{ij} \Psi_i^{pd,\sigma} \Psi_j^{\sigma,dp} + \sum J_{ij} [2\langle s_i s_j \rangle - \frac{n_i n_j}{2}] + \sum g_{ij} \delta_i \delta_j + H_{CDW} \quad (1)$$

where $\Psi_i^{pd,\sigma}$, $\Psi_j^{\sigma,dp}$ are quasiparticle Hubbard-like operators for the copper-oxygen singlet band, J_{ij} is the superexchange constant of the copper spin coupling and g_{ij} is a screened Coulomb repulsion of the doped holes, $1 + \delta_i = \sum_{\sigma} \Psi_i^{\sigma,\sigma} + 2\Psi_i^{pd,pd}$. The quasiparticle interaction H_{CDW} mediated by the phonon field leads to a CDW transition [6].

In addition to the usual mean field approach we have taken into account that anticommutators of Hubbard-like operators can be affected by the doping index level per one unit cell, spin magnetization and charge modulation (non-Fermi statistics effect (NFS)):

$$P_i^{\sigma} = \Psi_i^{pd,pd} + \Psi_i^{\sigma,\sigma} = \frac{1 + \delta_i}{2} + (-1)^{\frac{1}{2}-\sigma} s_i^z \quad (2)$$

The appearance of SDW we describe via the Fourier component:

$$s_{q_s}^z = \frac{1}{N} \sum s_i^z \exp(iq_s R_i), \quad (3)$$

where q_s is the instability wave vector with respect to SDW formation. CDW can be taken into account in the same way by introducing the Fourier component of doped holes:

$$e_{q_e} = \frac{1}{N} \sum \delta_i \exp(iq_e R_i) \quad (4)$$

where q_e is the instability wave vector with respect to CDW formation. It is easy to show that the homogeneous part (δ_0) of the doped hole function per one unit cell (δ_i) does not contribute to the expectation value e_q (i.e. $\delta_i = \delta_0 + e_i$). Generally the wave vectors of CDW (q_e) and SDW (q_s) can be different. Below we consider both as commensurate wave vectors $q_s = q_e = (\pi, \pi)$ and incommensurate wave vectors $q_s = q_e = (\pi \pm \varepsilon_x, \pi \pm \varepsilon_y)$.

Using Roth's decoupling procedure [7] in the framework of a linear approximation we can write:

$$\frac{\langle P_i^{\sigma} P_j^{\sigma} + \Psi_i^{\sigma,\bar{\sigma}} \Psi_j^{\bar{\sigma},\sigma} \rangle}{\langle P_j^{\sigma} \rangle} = \frac{1 + \delta_0}{2} \left[1 + \frac{4 \langle s_i s_j \rangle}{(1 + \delta_0)^2} \right] - \left(\langle \frac{e_i}{2} \rangle + (-1)^{\frac{1}{2}-\sigma} \langle s_i^z \rangle \right) \left[1 - \frac{4 \langle s_i s_j \rangle}{(1 + \delta_0)^2} \right] \quad (5)$$

where the angular brackets correspond to the thermodynamic expectation values. Then the equations of motion are written as:

$$\begin{aligned} i\hbar \frac{\partial}{\partial t} \Psi_k^{\sigma,pd} &= \varepsilon_k \Psi_k^{\sigma,pd} + \eta_{k+q}^{\sigma} \Psi_{k+q}^{\sigma,pd} \\ i\hbar \frac{\partial}{\partial t} \Psi_{k+q}^{\sigma,pd} &= \varepsilon_{k+q} \Psi_{k+q}^{\sigma,pd} + \eta_k^{\sigma} \Psi_k^{\sigma,pd} \end{aligned} \quad (6)$$

where

$$\begin{aligned} \eta_{k+q}^{\sigma} &= [t_{k+q} - \frac{4}{(1 + \delta_0)^2} \langle s_i s_j \rangle t_k] \\ &\langle \frac{e_q}{2} - (-1)^{\frac{1}{2}-\sigma} s_q^z \rangle + G_{k+q}^{\sigma} + G_k^{ph} \end{aligned} \quad (7)$$

and ε_k is the energy dispersion in the normal state. The CDW order parameter is determined by the relations [8]:

$$G_{k+q}^\sigma = -\frac{2}{(1+\delta_0)N} \sum_{k'} \{ j_{k'-k} \langle \Psi_{k'+q}^{pd,\bar{\sigma}} \Psi_{k'}^{\bar{\sigma},pd} \rangle + g_{k'-k} \langle \Psi_{k'+q}^{pd,\sigma} \Psi_{k'}^{\sigma,pd} \rangle \}, \quad (8)$$

$$G_k^{ph} = \sum_{\omega_q} [A(\omega_q) - B(\omega_q) \times \frac{(\hbar\omega_q)^2 \Theta(\hbar\omega_D - |\varepsilon_k|) \Theta(\hbar\omega_D - |\varepsilon_k - \varepsilon_{k+q}|)}{(\varepsilon_k - \varepsilon_{k+q})^2 - (\hbar\omega_q)^2}] \quad (9)$$

where $\omega_q = 40meV$ is the frequency of active phonon mode in the CDW transition.

The thermodynamic values of the Fourier component $\langle e_q \rangle$ and $\langle s_q \rangle$ are calculated self-consistently:

$$e_q = \frac{1}{2} \sum_k [\langle \Psi_{k+q}^{pd,\sigma} \Psi_k^{\sigma,pd} \rangle + \langle \Psi_{k+q}^{pd,\bar{\sigma}} \Psi_k^{\bar{\sigma},pd} \rangle] \\ s_q^z = \frac{1}{2} \sum_k [\langle \Psi_{k+q}^{pd,\bar{\sigma}} \Psi_k^{\bar{\sigma},pd} \rangle - \langle \Psi_{k+q}^{pd,\sigma} \Psi_k^{\sigma,pd} \rangle] \quad (10)$$

The correlation function is determined by

$$\langle \Psi_{k+q}^{pd,\sigma} \Psi_k^{\sigma,pd} \rangle = P \frac{\eta_{k+q}^\sigma}{E_{1k}^\sigma - E_{2k}^\sigma} [f(E_{1k}^\sigma) - f(E_{2k}^\sigma)] \quad (11)$$

with

$$E_{1k,2k}^\sigma = \frac{\varepsilon_k + \varepsilon_{k+q}}{2} \pm \frac{1}{2} [(\varepsilon_k - \varepsilon_{k+q})^2 + 4|\eta_{k+q}^\sigma|^2]^{1/2} \quad (12)$$

III. ENERGY DISPERSION AT LOW DOPING

The one band approach is usually valid for a large enough doping level. Therefore if δ goes to zero we explored the two band model for layered cuprates [2,9,10]. In this case the energy dispersion is:

$$\varepsilon_k = \frac{E_k^{dd} + E_k^{pp}}{2} + \frac{1}{2} [(E_k^{dd} - E_k^{pp})^2 + 4E_k^{dp} E_k^{pd}]^{1/2} \quad (13)$$

where

$$E_k^{dd} = \varepsilon_d + \sum [\frac{1-\delta_0}{2} + \frac{2}{(1-\delta_0)} \langle s_i s_j \rangle] t_{ij}^{12} \exp(ikR_{ij}) \quad (14)$$

$$E_k^{pp} = \varepsilon_p + \sum [\frac{1+\delta_0}{2} + \frac{2}{(1+\delta_0)} \langle s_i s_j \rangle] t_{ij}^{12} \exp(ikR_{ij}) \quad (15)$$

are dispersions of the lower Hubbard copper band and the singlet-correlated oxygen band, respectively and

$$E_k^{dp} = \sum [\frac{1+\delta_0}{2} - \frac{2}{(1-\delta_0)} \langle s_i s_j \rangle] t_{ij}^{12} \exp(ikR_{ij}) \quad (16)$$

$$E_k^{pd} = \sum [\frac{1-\delta_0}{2} - \frac{2}{(1+\delta_0)} \langle s_i s_j \rangle] t_{ij}^{12} \exp(ikR_{ij}) \quad (17)$$

describe their hybridization. If δ_0 goes to zero the spin dependent factors in E_k^{dd} and E_k^{pp} become zero due to antiferromagnetic correlations. At the same time, as one can see from the expressions for E_k^{pd} and E_k^{dp} the antiferromagnetic correlations enhance the interband coupling. So, at small doping level the energy dispersion will be determined by the expression

$$\varepsilon_k(\delta \rightarrow 0) = \frac{\varepsilon_d + \varepsilon_p}{2} + \frac{1}{2} \sqrt{(\varepsilon_p - \varepsilon_d)^2 + 16[t_1^{12}(\cos k_x + \cos k_y)]^2} \quad (18)$$

where t_1^{12} is a transfer integral between nearest neighbor copper sites. From (18) one can obtain that the bottom of the band corresponds to the point $(\frac{\pi}{2}, \frac{\pi}{2})$ of the Brillouin zone. This result coincides with experimental data [5]. We stress here that in contrast to Chubukov's model of the normal state of lightly doped cuprates [5] or slave boson approximations [11] any long range order is unnecessary in our two band approximation. The expression (18) is valid at $\langle s_i^z \rangle = 0$, i.e. for the usual paramagnetic phase.

IV. NUMERICAL RESULTS AND DISCUSSION

The spectral weight of the singlet band changes with doping level δ (hole concentration per one unit cell of bilayer) as $2\delta/(1+\delta)$. Thus, the condition of half-filling (which approximately corresponds to the optimal doping level) yields $\delta_{opt} = 1/3$. Because the bilayer unit cell contains two copper sites we conclude that T_c has a maximum near hole concentrations $x \approx 1/6$ per one copper site.

The evolution of the Fermi surface for three doping levels are presented in Fig.1. With decreasing doping level the Fermi surface shrinks to the pockets near the point $(\frac{\pi}{2}, \frac{\pi}{2})$ of the Brillouin zone.

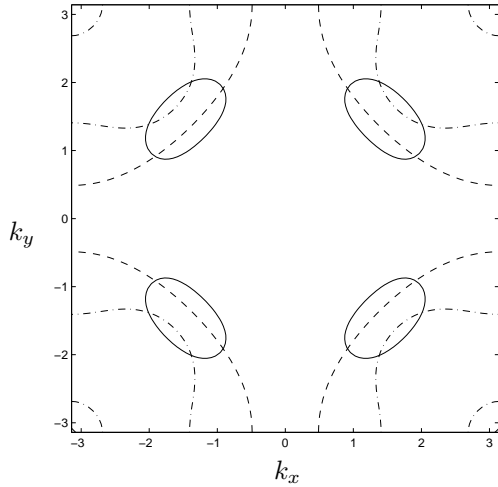


FIG. 1. Evolution of the Fermi surface of the singlet band for three doping levels; $x = 0.025$ (solid curve), $x = 0.09$ (dash-dotted) and $x = 0.17$ (dashed).

This behavior qualitatively agrees with photoemission experimental data [3,4] and provides a good basis for the analysis of Peierls like instabilities, which as it was pointed out by many authors [6,12,13], is very sensitive to the topological properties of the Fermi surface.

Numerical solutions of the equations (8)-(10) are shown in Fig. 2.

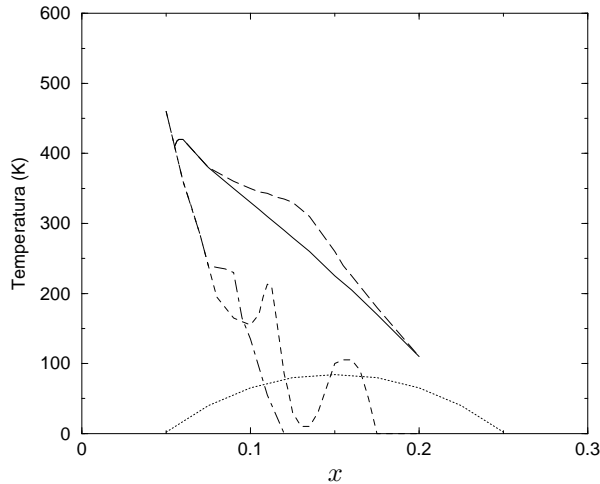


FIG. 2. Critical temperatures vs. doping; T_d^* (CDW) - long dashed curve, T_d^* (SDW) - solid curve, T_s^* (CDW) - dashed-dotted, T_s^* (SDW) - short dashed. The parabola corresponds to the superconducting transition temperature T_c (schematically).

The values of hopping integrals in the one band approximation were chosen between first, second and third neighbors as $t_1 = 72.5$, $t_2 = 0$ and $t_3 = 12$ (in meV) respectively. The set of other used parameters is presented in Table 1.

Table 1. The values of spin-spin correlation function and superexchange plus Coulomb screening integral at different doping level

x	$\langle S_i S_j \rangle$	$J_0 + G_0$ (meV)
0.20	-0.0381	160
0.15	-0.0728	225
0.10	-0.1287	320
0.05	-0.2301	320

The short range interactions (superexchange and screened Coulomb repulsion), as a rule, yield the d-wave order parameters of CDW and SDW, whereas NFL-effects, together with phonon mediated interaction, lead to a anisotropic s-wave pseudogap component. In general the calculated CDW and SDW order parameters have $s + id$ symmetry and the temperature dependence of s- and d-components are different. The critical temperature of the d-component (T_d^*) is always higher than T_s^* at all considered doping levels. Both types of solutions (CDW or SDW) display the correct doping dependence. In according to photoemission data [3,4] and NMR [14] the critical temperature of the pseudogap goes down when the doping decreases. The phase diagram of superconductivity (parabolic line) is given schematically as in [14]. From Eqs. (8), (11) it is clear that the critical temperature of the d- component CDW (T_d^*) is not sensitive to the external magnetic field. This result agrees well with recent experimental observation [15]. Calculated mean field critical temperatures of CDW (T_d^*) are higher than for SDW in the complete doping range. This result is also consistent with the widely accepted opinion that a transition towards the so called "stripe" phase in underdoped cuprates are charge rather than spin driven [16].

In Fig.3 we show the magnitude of the instability wave vector $Q = (\pi \pm \varepsilon_x, \pi \pm \varepsilon_y)$ vs. doping index. We have found the maximum of ε_y around $x_{CDW} \sim 0.09$ for CDW and $x_{SDW} \sim 0.11$ for SDW. It would be interesting to check our theoretical conclusion experimentally.

It is easy to see from Eq. (10) that for a d-wave order parameter with pure commensurate wave vector $q = Q = (\pi, \pi)$ both expectation values $\langle s_q \rangle$ and $\langle e_q \rangle$ vanish, but they are finite when the wave vector Q becomes incommensurate. Because in general the order parameters are complex, the expectation values $\langle s_q \rangle$ and $\langle e_q \rangle$ have real and imaginary components. Its values at the superconducting transition temperature are presented in Fig.4.

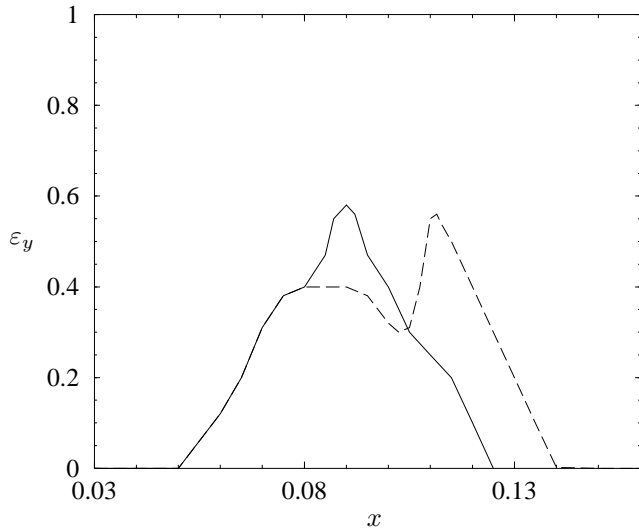


FIG. 3. The variation of incommensurability component ε_y vs. doping index; for CDW- solid and for SDW - dashed curve, respectively.

The real component $\langle e_q \rangle$ is about 0.1 – 0.15 at temperatures $T \geq T_c$ and disappears at T_s^* .

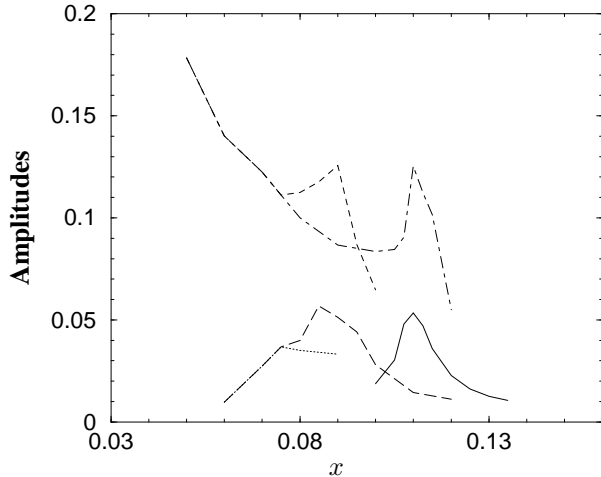


FIG. 4. Calculated values $\langle e_q \rangle$ and $\langle s_q \rangle$ for temperatures around T_c ; $Re \langle e_q \rangle$ (CDW)-dashed curve, $Re \langle e_q \rangle$ (SDW) - dotted-dashed, $Im \langle s_q \rangle$ (SDW) - solid, $Im \langle e_q \rangle$ (CDW) -long dashed, $Im \langle e_q \rangle$ (SDW) -dotted.

The imaginary parts of $\langle s_q \rangle$ and $\langle e_q \rangle$ in general are about 0.01 – 0.05 and stay up to T_d^* and then drastically vanish.

V. CONCLUSION

To conclude we have calculated Fourier amplitudes of CDW and SDW order parameters in underdoped cuprates. Our calculation provides an explanation for the

experimentally observed evolution of the Fermi surface and the doping dependence of the pseudogap formation temperature. The charge instability preforms the spin instability and the incommensurability has the maximum at $x \sim 0.1$ holes per one copper site. We hope our present calculations will help in better understanding many of the strange features in the shape and linewidth of NMR in layered cuprates.

Acknowledgments: We would like to thank G.Seibold for helpful comments and a critical reading of the manuscript. This work is supported in part by INTAS, Grant 96-0393. One of us (I.Eremin) is grateful for the financial support to Russian Ministry of Education (Grant No. 97-0-8.1-7133) and to the research program of the International Center for Fundamental Physics in Moscow (INTAS Grant 96-0457).

-
- [1] J. Haase, N.J.Curro, R.Stern, C.Milling, C. P. Slichter, B. Dabrowskii, D. Hinks, and O. Schirmer, Program and Abstracts of Colloquium on Magnetic Resonance in High-Tc Superconductors, Engelberg, Switzerland, Jan., 17-21, 1999.
 - [2] M.V. Eremin, S. G. Solovjanov, and S.V. Varlamov, J. Phys. Chem. Solids, Vol.56, 1713 (1995); M.V. Eremin, S. G. Sololjanov, S. V. Varlamov, D. Brinkmann, M.Mali, R. Markendorf, and J.Roos, JETP Lett. 60, 125 (1994).
 - [3] A. G. Loeser, Z.-X. Shen, D. S. Dessau, D. S. Marshall, C. H. Park, P. Fournier, A. Kapitulnik, Science 273, 325 (1996).
 - [4] H. Ding, T. Yokoya, J. C. Campuzano, T. Takahashi, M. Randeria, M. R. Norman, T. Mochiku, K. Kadowaki, and J. Giapintzakis, Nature (London)382, 51 (1996).
 - [5] S. LaRosa, I. Vobornik, F. Zwick, H. Berger, M. Grioni, G.Margaritondo, R.J.Kelley, M. Onnellion, and A. Chubukov, Phys. Rev. B 58, R525 (1997).
 - [6] I. Eremin, M. V. Eremin, S. V. Varlamov, D. Brinkmann, M.Mali, and J. Ross; Phys. Rev. B56, 11305 (1997).
 - [7] L. M. Roth, Phys. Rev. 184, 451 (1969).
 - [8] S. V. Varlamov, M. V. Eremin, and I. M. Eremin; JETP Lett. 66, 569 (1997).
 - [9] N.M.Plakida, R.Hayn and J.L.Richard, Phys.Rev.B 51, 16599 (1995).
 - [10] M. V. Eremin, S. G. Solov'yanov, and S. V. Varlamov, JETP. 85 (5),p.963-967, (1997).
 - [11] M.U. Ubbens, P. Lee, Phys. Rev. B 46, 8434 (1992).
 - [12] R.S.Markiewicz, Phys. Rev. B56, 9091 (1997)
 - [13] F.Onufrieva, P.Pfeuty, and M.Kiselev, Phys. Rev. Lett. 82, 2370 (1999).
 - [14] G.V.M.Williams , J.L.Tallon, R.Michalak and Dupree, Phys.Rev.B 54, R6909 (1996).
 - [15] K.Gorny, O.M.Vyaselev, J.A. Martindale, V.A. Nandor, C.H.Pennington, P.C.Hammel, W.L.Hults, J.L.Smith, P.L.Kuhns, A.P.Reyes, and W.G.Moulton, Phys. Rev. Lett 82, 177 (1999).
 - [16] O.Zachar, S.A.Kivelson, V.J.Emery, Phys.Rev.B 57,1422 (1998).